Morphometric features of corneal epithelial basal cells, and their relationship with corneal nerve pathology and clinical factors in patients with type 2 diabetes

Fukashi Ishibashi*, Asami Kawasaki, Emi Yamanaka, Aiko Kosaka, Harumi Uetake

ABSTRACT

Aims/Introduction: We compared the morphometric features of corneal epithelial basal cells between patients with type 2 diabetes mellitus and healthy controls, and analyzed the relationship of these features with corneal nerve fiber pathology and clinical factors in the patients.

Materials and Methods: Corneal epithelial basal cells and corneal nerve fibers were visualized by corneal confocal microscopy in 75 patients with type 2 diabetes and 42 age-matched controls. Density, area and area variability of corneal epithelial basal cells, as well as the width of the intercellular space between neighboring cells, were evaluated for both groups.

Results: Patients showed decreased density ($P < 0.02$) and area ($P < 0.0001$), larger area variability ($P < 0.0001$) and a wider intercellular space ($P < 0.0001$) compared with controls. Density correlated inversely with area ($P < 0.0001$), width of intercellular space ($P < 0.03$) and beading frequency ($P < 0.03$), whereas it correlated directly with prothrombin time ($P < 0.002$) and activated partial thromboplastin time ($P < 0.03$). Area correlated inversely with duration of diabetes ($P < 0.05$) and coefficient of variation of area ($P < 0.01$), whereas it correlated directly with beading frequency ($P < 0.05$). Area variability correlated inversely with area ($P < 0.01$) and prothrombin time ($P < 0.01$), whereas it correlated directly with fibrinogen level ($P < 0.0001$).

Conclusions: Type 2 diabetes induces morphometric changes in corneal epithelial basal cells; this seems to be related to the morbid period of diabetes, beading frequency of corneal nerve fibers and blood coagulation state. (J Diabetes Invest, doi: 10.1111/jdi.12083, 2013)

KEY WORDS: Confocal microscopy, Corneal epithelial basal cell, Type 2 diabetes mellitus

INTRODUCTION

Patients with diabetes mellitus often have diabetic keratoepitheliopathy[1], such as punctate keratitis, recurrent corneal erosion, persistent epithelial defects and corneal endothelial damage[2–4]. Furthermore, the additional stress related to procedures carried out frequently in diabetic patients, such as cataract surgery, vitrectomy and photocoagulation, induces diabetic keratoepitheliopathy[5].

The cornea is the most innervated peripheral human tissue in the body (300–500 times the innervation of the skin), and it receives sensory and autonomic nerve fibers[6] (NFs) that have free endings between the epithelial cells. These NFs have an important influence on corneal trophism and contribute to the maintenance of a healthy corneal surface, thus playing a pivotal role in protecting the eyes[7].

Patients with diabetes have decreased corneal sensitivity and tear secretion, and are prone to dry eye[8]. Although a decreased density of corneal epithelial basal cells (CEBCs) has been reported in patients with diabetes[9,10], a detailed morphometric analysis of CEBCs in such patients and the relationship of these morphometric features with pathological changes in corneal NFs beneath CEBCs have never been reported. Furthermore, few studies have examined the contribution of systemic factors to pathological changes in CEBCs[11].

Non-invasive corneal confocal microscopy (CCM) enables the visualization of CEBCs, as well as the corneal NFs beneath CEBCs, in a clinical setting. In the present study, density, area and area variability of CEBCs, as well as the width of the intercellular space between neighboring cells, were evaluated using CCM and compared between patients with type 2 diabetes and healthy controls. These morphometric features of CEBCs correlated with systemic factors and corneal NF pathology in type 2 diabetic patients.

MATERIALS AND METHODS

Patients with type 2 diabetes who were visiting Ishibashi Clinic for the first time were invited to participate along with age-matched volunteers without diabetes (controls; glycated

Ishibashi Clinic, Hiroshima, Japan
*Corresponding author. Fukashi Ishibashi Tel.: +0829-32-5206 Fax: +0829-32-7553
E-mail address: ishiclic@urban.ne.jp
Received 17 November 2012; revised 9 February 2013; accepted 26 February 2013

hemoglobin [HbA_{1c}] <5.7%; fasting plasma glucose <5.5 mmol; or casual postprandial plasma glucose <7.7 mmol). Exclusion criteria included the following: alcohol consumption >20 g/day, presence of neuropathy because of another etiology, contact lens use, or taking any anti-coagulant or anti-platelet agents. Written informed consent was obtained from all participants before participation. The protocol of the recent research was approved by the ethics committee of Ishibashi Clinic.

Corneal Confocal Microscopy

Participants were examined using a Heidelberg Retina Tomograph 3 equipped with a Rostock Cornea Module (Heidelberg Engineering, Heidelberg, Germany), as reported previously[12]. Briefly, each examined eye was anesthetized with one drop of 0.4% benoxinate hydrochloride (Santen Pharmaceutical Co., Osaka, Japan). A drop of Comfort Gel (Dr. Mann Pharma, Berlin, Germany) was applied to the tip of the lens, and a disposable sterilized Tomocap was mounted on the holder to cover the objective lens. After applying Comfort Gel to the Tomocap, the lens was slowly advanced forward until the gel touched the cornea. After focusing on CEBCs, two to three clear images of CEBCs were obtained, followed by four to five fine images of the nerve plexus layer (sub-basal layer). The density of CEBCs (/mm^2) was determined using the cell counter attached to the CCM apparatus. At first, the region of interest (ROI; mm^2) was defined, and all cells in the ROI were marked (cell number). Then, cell density was automatically calculated (cells/mm^2; Figure 1a). To assess the area of an individual CEBC, the inner rim of intercellular space was traced and the loop was closed. Thereafter, the number of pixels in the loop was counted using Photoshop Elements 8.0 (Adobe Systems Inc., San Jose, CA, USA) after smoothing and enlarging five times by PhotoZoom Pro4 (BenVista Ltd., Houston, TX, USA; Figure 1b). The method for determination of width (μm) of the intercellular space between neighboring CEBCs is shown in Figure 1c. The raw image of CEBC was processed by Photozoom Pro4, and opened as a .jpg file in Simple PCI (Compix Inc., Cranberry Township, PA, USA). The outer and inner rims were traced continuously, and the loop was closed. After 80 tracings of intercellular space for each participant, the mean breadth of each intercellular space was calculated simultaneously by breadth measurement function of Simple PCI.

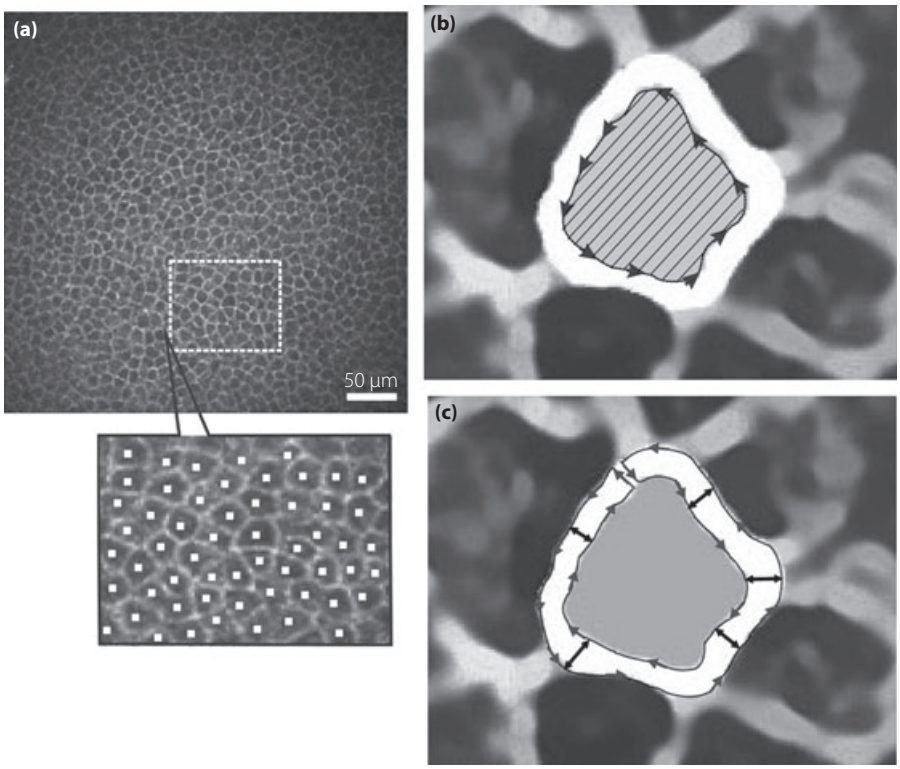

Figure 1 | (a) The determination of the density of corneal epithelial basal cells (CEBCs). At first, the region of interest (ROI; mm^2) was arbitrarily defined, and all cells in the ROI were marked (cell number). Then, cell density (cells/mm^2) was automatically calculated. (b) The measurement of the area of CEBCs. The inner rim of intercellular space was traced and the loop was closed. Then, the number of pixels in the loop (hatched area) was counted using Photoshop Elements 8.0 (Adobe Systems Inc., San Jose, CA, USA) after smoothing and enlarging five times by PhotoZoom Pro4 (BenVista Ltd., Houston, TX, USA). (c) The determination of the breadth of the intercellular space between neighboring CEBCs. After smoothing and enlarging by Photozoom Pro4, images were opened as jpg file in Simple PCI (Compix Inc., Cranberry Township, PA, USA). The outer and inner rims were traced carefully and the loop was closed. After 80 tracings of intercellular space for each participant, the mean breadth of each intercellular space was calculated simultaneously by breadth measurement function of Simple PCI.

The collected images of the sub-basal nerve plexus were used to quantify the following parameters for defining corneal NF changes: (i) corneal NF density/mm^2 (CNFD); (ii) corneal NF length mm/mm^2 (CNFL); (iii) corneal NF branch density/mm^2 (CNBD); (iv) length of the corneal nerve branch mm/mm^2 (CNBL) emanating from the major nerve trunk; (v) tortuosity; and (vi) frequency (/0.1 mm) of beading. All measurements, except for tortuosity, were determined using Image J (Texelcraft, Tokyo, Japan). Tortuosity was determined according to the grading system proposed by Oliveira-Soto and Efron[13].

Assessment of Nerve Function

Current perception threshold (CPT) and vibration perception threshold (VPT) were measured as reported previously[12] using a Neurometer (Neurotron, Baltimore, MD, USA) and a biothesiometer (Bio-Medical Instruments, Newbury, OH, USA), respectively. The lowest stimulus that the participant could perceive was defined as CPT for that current frequency in each individual. To determine VPT, eight readings were obtained and averaged.

Assessment of Diabetic Neuropathy

Diabetic neuropathy (DN) was diagnosed in patients with type 2 diabetes according to the presence of two of the following three factors recommended in the simplified diagnostic criteria proposed by the Japanese Study Group of Diabetic Neuropathy[14]: (i) subjective symptoms of bilateral lower limbs or feet; (ii) loss of or decreased ankle jerk; and (iii) abnormal VPT assessed using a C128 tuning fork. As shown in Table 1, 18 of 75 patients had DN. No significant difference in age (59.4 ± 1.9 vs 54.4 ± 1.6 years), body mass index (BMI; 25.2 ± 0.7 vs 26.9 ± 0.9 kg/m^2) and HbA_{1c} level (9.0 ± 0.41 vs 9.1 ± 0.27%) was observed between patients with or without DN, whereas the morbid period was longer (13.6 ± 2.5 vs 6.7 ± 0.84 years) in patients with DN than in those without.

Laboratory Data

At the first visit, HbA_{1c} levels (converted to National Glycohemoglobin Standardization Program units by adding 0.4% to the measured values)[15], blood urea nitrogen, creatinine, lipids levels, plasma fibrinogen, activated partial thromboplastin time (APTT) and prothrombin time (PT-INR; prothrombin time-international normalized ratio) were determined.

Statistical Analysis

All statistical analyses were carried out using the SPSS medical package (SPSS, Chicago, IL, USA). Data are presented as mean ± standard error of the mean. Analysis of variance (ANOVA) was used to compare controls and type 2 diabetic patients with or without DN. The correlation of the morphometric features of CEBCs with corneal NF pathology and clinical data in the type 2 diabetic patients was assessed by multiple regression analysis, with the morphometric features of CEBCs as outcome variables, and NF pathology and clinical data as

Table 1 | Clinical characteristics of control subjects and type 2 diabetic patients with or without diabetic neuropathy

	Control subjects	Type 2 diabetic patients	Without neuropathy	With neuropathy
n (male/female)	42 (25/17)	75 (54/21)	57 (41/16)	18 (13/5)
Age (years)	53.1 ± 1.8	55.6 ± 1.3	54.4 ± 1.6	59.4 ± 1.9
BMI (kg/m^2)	22.4 ± 0.5	26.5 ± 0.7***	26.9 ± 0.9	25.2 ± 0.7
SBP (mmHg)	131.8 ± 1.4	148.4 ± 1.9***	148.7 ± 2.2	147.3 ± 3.8
DBP (mmHg)	81.1 ± 0.6	88.7 ± 0.7***	89.2 ± 0.8	87.0 ± 1.6
No. treated with ARB/ACEI (%)	6 (14.3)	13 (17.3)	10 (17.5)	5 (27.8)
HbA_{1c} (%)	5.7 ± 0.06	9.1 ± 0.22***	9.1 ± 0.27	9.0 ± 0.41
LDL-C (mmol/L)	2.75 ± 0.10	3.40 ± 0.11**	3.47 ± 0.13	3.15 ± 0.17
No. treated with statins (%)	5 (11.9%)	14 (18.7)	10 (17.5)	4 (22.2)
HDL-C (mmol/L)	1.88 ± 0.075	1.46 ± 0.044**	1.49 ± 0.05	1.34 ± 0.074
Triglycerides (mmol/L)	0.94 ± 0.10	2.59 ± 0.31***	2.57 ± 0.339	2.66 ± 0.843
ACR (mg/gCr)	7.0 ± 1.9	234.9 ± 104.2	106.1 ± 40.3	642.8 ± 417.6
eGFR (mL/min)	78.7 ± 2.7	88.1 ± 3.1	89.1 ± 3.5	84.9 ± 7.0
APTT (min)	32.4 ± 0.6	30.1 ± 0.44*	30.0 ± 0.54	30.4 ± 0.75
PT-INR	1.11 ± 0.02	1.02 ± 0.01***	1.01 ± 0.01	1.05 ± 0.03
Fibrinogen (mg/dL)	237.9 ± 7.3	289.3 ± 12.9*	284.0 ± 12.8	306.3 ± 36.9
Duration of diabetes (years)		8.4 ± 0.92	6.7 ± 0.84	13.6 ± 2.5##

Data are the mean ± standard error of the mean in control subjects and patients with type 2 diabetes with or without diabetic neuropathy (DN). *P < 0.01, **P < 0.001, ***P < 0.0001 compared with control subjects; ##P < 0.01 compared with type 2 diabetic patients without DN. Statistical analyses were carried out with analysis of variance. To standardize glycated hemoglobin (HbA_{1c}) values to National Glycohemoglobin Standardization Program units, 0.4% was added to the measured HbA_{1c} values. ACEI, angiotensin-converting enzyme inhibitor; ACR, urinary albumin/creatinine ratio; APTT, activated partial thromboplastin time; ARB, angiotensin receptor blocker; BMI, body mass index; DBP, diastolic blood pressure; eGFR, estimated glomerular filtration rate; HDL-C, high-density lipoprotein-cholesterol; LDL-C, low-density lipoprotein-cholesterol; PT-INR, prothrombin time-international normalized ratio; SBP, systolic blood pressure.

predictor variables. Receiver operating characteristic (ROC) analysis established cut-off levels for CEBC density, CEBC area, CEBC area variability, and width of the intercellular space between controls and type 2 diabetic patients. Sensitivity and specificity were equally weighted. A *P*-value of <0.05 was considered statistically significant.

RESULTS

Table 1 shows the clinical and demographic data of controls and type 2 diabetic patients with or without DN. BMI, systolic and diastolic blood pressure, HbA_{1c}, low-density lipoprotein cholesterol, triglycerides, and fibrinogen levels were significantly higher, whereas high-density lipoprotein cholesterol, APTT and PT-INR were significantly lower in type 2 diabetic patients than in controls.

When nerve function was assessed in terms of CPT (Figure 2a) and VPT (Figure 2b), CPT at 2,000, 250 and 5 Hz was significantly higher in diabetic patients than in controls, as was VPT. The development of DN further increased CPT of all frequencies, as well as VPT.

Figure 3 shows the representative CEBCs in a control subject and a patient with type 2 diabetes. Compared with the control, the patient had visibly smaller CEBCs.

Sensitivity and specificity of CEBC morphometric features obtained by CCM examination were assessed using an ROC curve (Figure 4). For the examination of morphological changes of CEBCs using CCM, the sensitivity, specificity, and tentative cut-off level between controls and type 2 diabetic patients were as follows: 61.0, 70.7% and 5,765/mm^2, respectively, for density; 93.1, 92.0% and 163.5 μm^2, respectively, for area; 86.7, 96.6 and 21.8%, respectively, for coefficient of variation (CV) of CEBC area; and 86.7, 83.9% and 2.28 μm, respectively, for width of intercellular space. The type 2 diabetics showed decreased density, smaller area, increased area variability and a wider intercellular space compared with controls. In contrast, there was no significant difference in any of these features between patients with or without DN (Figure 5). Then, the influence of diabetic nephropathy and retinopathy on morphometric parameters of CEBCs was examined. The multiple regression analysis showed no significant correlation between AER (P = 0.463–0.892) or eGFR (P = 0.157–0.493) and morphometric features of CEBCs. There was no significant difference (P = 0.282–0.739) in these features between patients with diabetic retinopathy (n = 17) and those without (n = 58).

When morphological parameters of corneal sub-basal NF were compared among controls and type 2 diabetics with or without DN, type 2 diabetic patients showed decreased CNFD and CNFL, and the development of DN further impaired these values. CNBD was lower in type 2 diabetic patients than in controls; however, there was no difference between patients with DN and those without. Furthermore, an increase in tortuosity and a decrease in beading frequency were observed in

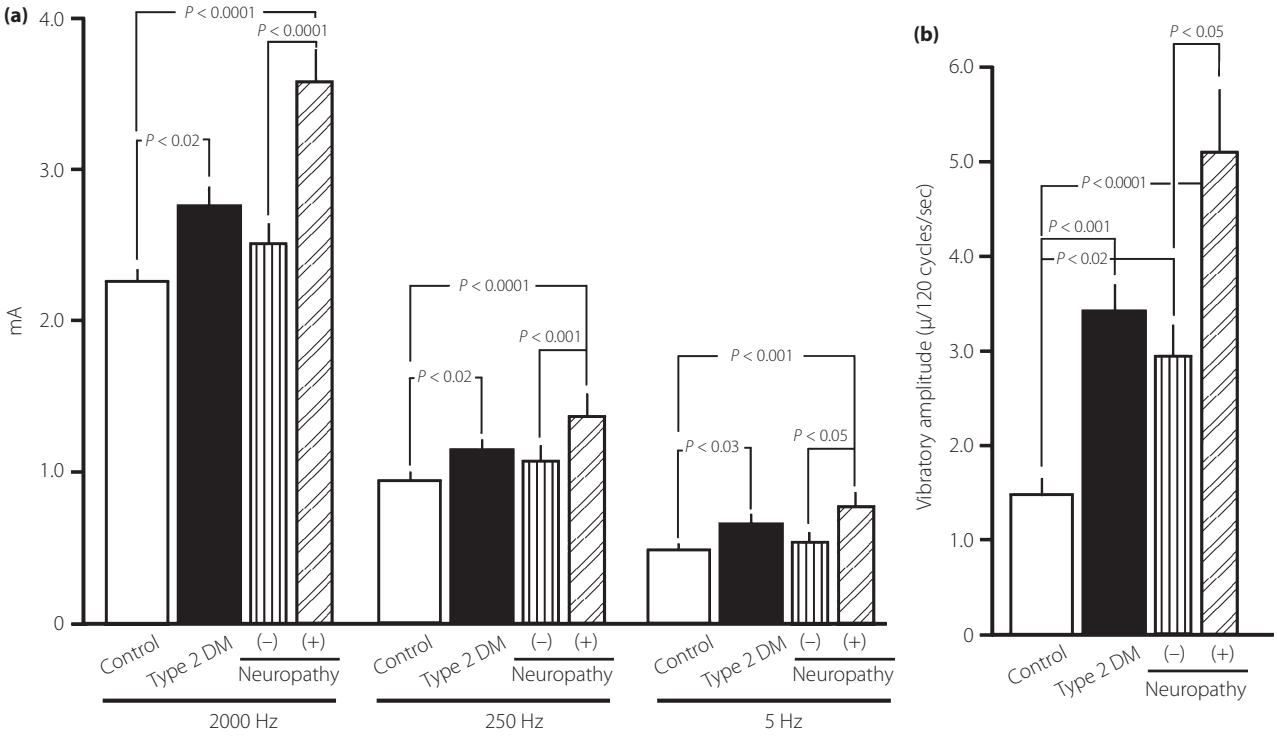

Figure 2 | (a) Comparison of current perception threshold (CPT) at three different frequencies (2000, 250 and 5 Hz) and (b) vibration perception threshold (VPT), expressed as absolute amplitude at 120 cycles/s, between controls and type 2 diabetic patients (T2DM) with or without diabetic neuropathy (DN). Data are presented as mean ± standard error of the mean.

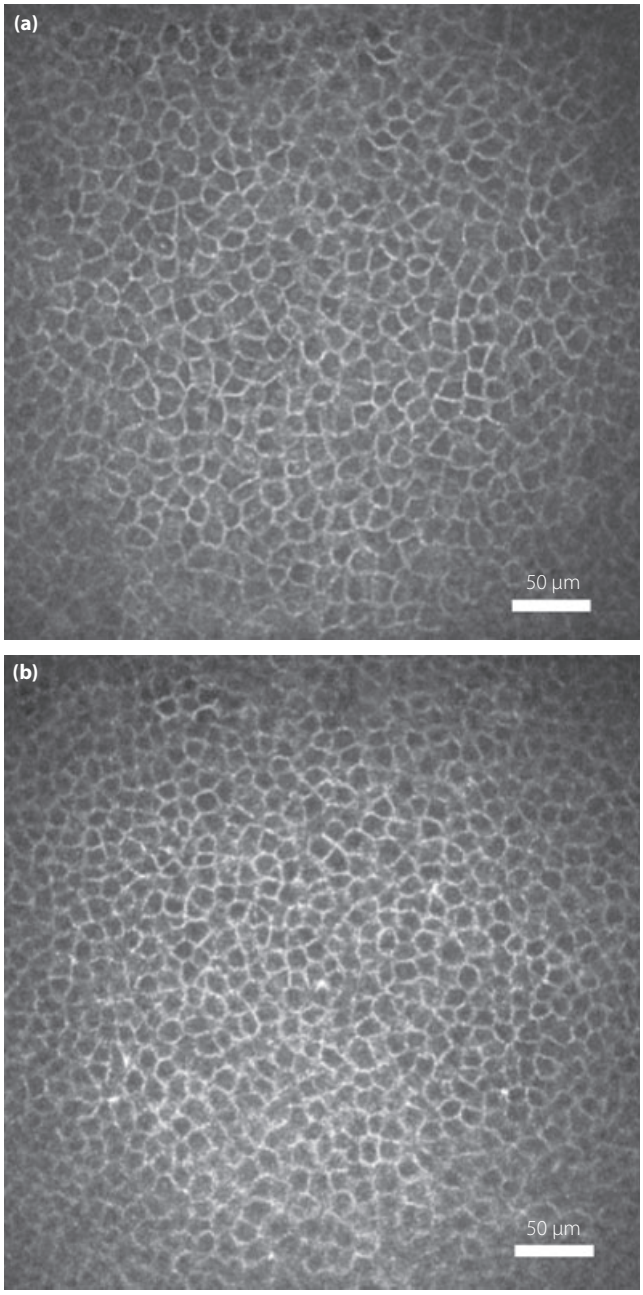

Figure 3 | (a) Confocal microscopic image of corneal epithelial basal cells (CEBCs) in a 43-year-old healthy subject with normal current perception threshold (CPT), normal vibration perception threshold (VPT) and normal parameters of the nerve plexus by corneal confocal microscopy (CCM). (b) CEBCs from a 45-year-old patient with type 2 diabetes who did not have diabetic neuropathy, and had normal CPT and increased VPT. The smaller CEBCs are shown.

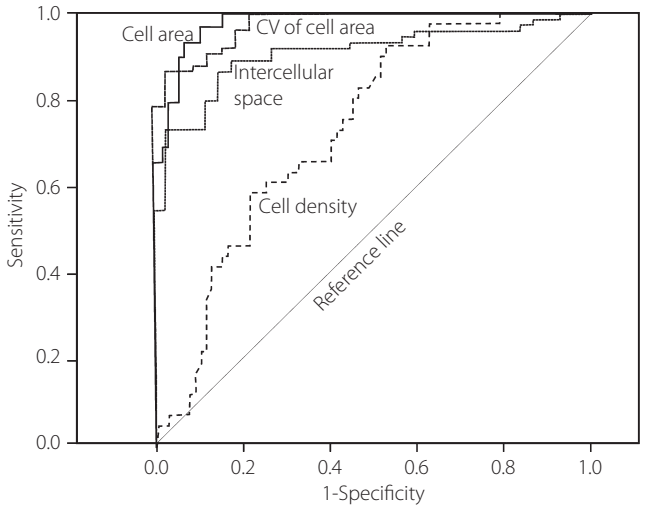

Figure 4 | Receiver operating characteristic (ROC) curves establishing cut-off levels between controls and type 2 diabetic patients for size of corneal epithelial basal cells (CEBCs), density of CEBCs, coefficient of variation (CV) of CEBC area and width of intercellular space, all of which were visualized by corneal confocal microscopy (CCM). Data were analyzed by Photoshop Elements 8.0 (Adobe Systems Inc. San Jose, CA, USA) and Simple PCI (Compix Inc. Cranberry Township, PA, USA).

diabetic patients compared with those in control subjects. The development of DN increased tortuosity (Table 2).

Multiple regression analysis showed that CEBC density changed in relation to PT-INR and APTT, and had an inverse relationship with CEBC area and intercellular space of CEBCs, and the beading frequency of corneal NFs. Beading frequency of the corneal NFs was a positive predictor, whereas the morbid period and area variability were negative predictors for CEBC area. CEBC area variability was inversely related with CEBC area and PT-INR, whereas high fibrinogen levels increased CEBC area variability. The intercellular space between neighboring CEBCs was inversely correlated with cell density (Table 3).

When the same analysis was carried out in non-diabetic control subjects, PT-INR was a positive predictor for CEBC density ($\beta = 0.396$, $P = 0.0046$), whereas CEBC area variability had a significant relationship with fibrinogen levels ($\beta = 0.492$, $P = 0.0012$).

DISCUSSION

The incidence of keratoepitheliopathy has been reported to be 22.8% in Japanese patients with diabetes and 8.5% in their non-diabetic counterparts[11], indicating that keratoepitheliopathy is a major ocular complication of diabetes mellitus. Furthermore, this can be a vision-threatening complication. The characteristic clinical features of keratoepitheliopathy include persistent corneal epithelial defects, delayed re-epithelialization and recurrent corneal erosion. Diabetic keratoepitheliopathy is a serious complication of intraocular surgery. In particular, corneal epithelial debridement carried out during vitreous surgery often results in prolonged corneal epithelial defects in patients with diabetes and interferes with vision. Despite the increase in diabetic patients and their intraocular surgery, the pathogenesis of diabetic keratoepitheliopathy remains to be fully disclosed.

CEBCs play a pivotal role in maintaining the morphological and functional integrity of not only corneal epithelial layer, but

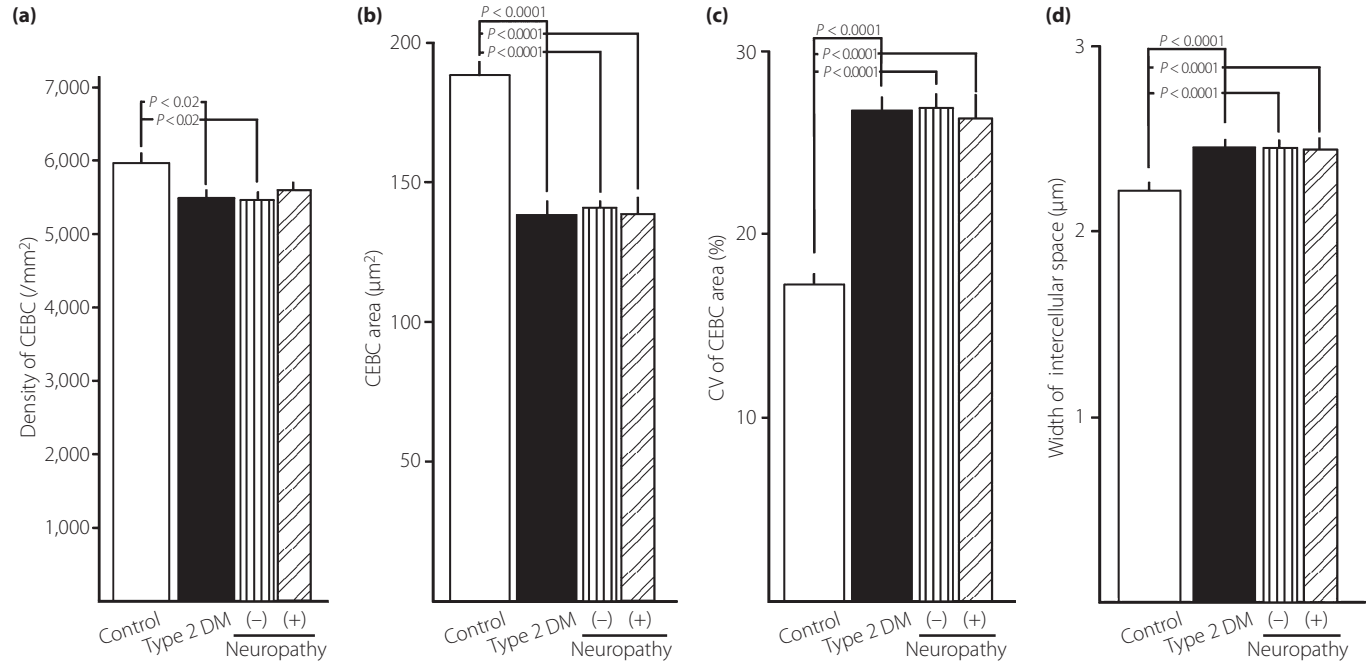

Figure 5 | Comparison of the (a) density of corneal epithelial basal cells (CEBCs), (b) area of CEBCs, (c) coefficient of variation (CV) of CEBC area and (d) width of intercellular space between neighboring CEBCs among controls and type 2 diabetic patients (T2DM) with (+) or without (–) diabetic neuropathy (DN) assessed by the simplified diagnostic criteria[14] proposed by the Japanese Study Group of Diabetic Neuropathy. CEBCs were visualized by corneal confocal microscopy (CCM) and analyzed by Photoshop Elements 8.0 (Adobe Systems Inc. San Jose, CA, USA) and Simple PCI (Compix Inc. Cranberry Township, PA, USA). Values are presented as mean ± standard error of the mean. The significance of differences between groups was determined by analysis of variance.

Table 2 | Comparison of morphological parameters of corneal nerve plexus observed by corneal confocal microscopy between control subjects and type 2 diabetic patients without or with diabetic neuropathy

	Control subjects	Type 2 diabetic patients	Without neuropathy	With neuropathy
Corneal nerve fiber density (/mm^2)	35.5 ± 2.2	26.9 ± 0.69***	28.42 ± 0.70‡	21.9 ± 1.23$^{\#}$
Corneal nerve fiber length (mm/mm^2)	13.3 ± 0.81	10.5 ± 0.26***	11.0 ± 0.30†	8.9 ± 0.29$^{\#}$
Corneal nerve branch density (/mm^2)	13.8 ± 1.1	9.31 ± 0.58**	9.46 ± 0.67†	8.85 ± 1.20
Corneal nerve branch length (mm/mm^2)	2.23 ± 0.17	2.10 ± 0.10	2.12 ± 0.11	2.02 ± 0.23
Tortuosity grade	1.73 ± 0.06	2.51 ± 0.05***	2.43 ± 0.05‡	2.78 ± 0.09$^{\#\#}$
Beading frequency (/0.1 mm)	29.9 ± 0.97	19.5 ± 0.36***	19.3 ± 0.42‡	20.0 ± 0.77

Data are mean ± standard error of the mean in control subjects and whole type 2 diabetic patients or subdivided by diabetic neuropathy. **$P < 0.001$, ***$P < 0.0001$ compared with control subjects; $^{†}P < 0.002$, $^{‡}P < 0.0001$ compared with control subjects; $^{\#}P < 0.05$, $^{\#\#}P < 0.01$ compared with type 2 diabetics without diabetic neuropathy. Statistical analyses were carried out with analysis of variance.

also endothelial cells[16]. The recent application of CCM to observe the cornea enables a thorough quantitative analysis of CEBCs.

In the present study, a quantified morphometric analysis of CEBCs and corneal NFs in type 2 diabetic patients was carried out using CCM, and the findings were compared with those of age-matched controls.

CEBC density in the controls (5,988 ± 100/mm^2) in the present study was quite similar to that reported previously by Castillo *et al.*[7] (5,858 ± 702/mm^2) and Quadrado *et al.*[9] (5,950 ± 653/mm^2). CEBCs are columnar with dimensions of 10 × 18 μm in fixed corneal preparations. CEBC area as estimated by slit-scanning confocal microscopy[17] in normal subjects was reported as 192 ± 19.6 μm^2, which is similar to that reported in the present study (188.2 ± 4.1 μm^2). A recent detailed morphometric analysis of CEBCs using CCM in control subjects showed that the mean individual CEBC area was constant when more than 40 CEBCs were measured[18]. As we measured 80 CEBCs in each participant, the variability in estimating the area of each CEBC reached sufficient reliability. CV of CEBC

Table 3 | Correlation between morphological parameters of corneal epithelial basal cells and corneal nerve pathology or clinical measures

	Density of CEBC		CEBC area		CV of CEBC area		Intercellular space of CEBC	
	β	*P*	β	*P*	β	*P*	β	*P*
Age	0.256	0.085	−0.195	0.172	−0.193	0.181	−0.054	0.720
BMI	0.167	0.252	−0.220	0.131	−0.178	0.221	0.130	0.381
Duration of type 2 diabetes	−0.003	0.980	−0.273	0.035	0.055	0.674	0.049	0.719
HbA_{1c}	−0.123	0.319	0.032	0.790	0.073	0.545	−0.013	0.921
SBP	−0.075	0.572	0.198	0.169	−0.10	0.940	−0.010	0.943
Density of CEBC			−0.657	0.0001	−0.155	0.196	−0.273	0.025
CEBC area	−0.706	0.0001			−0.333	0.007	0.192	0.133
CV of CEBC area	−0.158	0.196	−0.310	0.007			0.041	0.738
Intercellular space of CEBC	−0.261	0.025	0.171	0.133	0.041	0.738		
Corneal nerve fiber density	−0.115	0.355	−0.033	0.783	0.076	0.548	0.130	0.306
Corneal nerve fiber length	−0.103	0.411	−0.059	0.628	0.123	0.345	0.182	0.156
Corneal nerve branch density	−0.115	0.355	−0.080	0.512	0.069	0.597	0.201	0.142
Corneal nerve branch length	0.212	0.104	−0.092	0.469	0.164	0.209	0.204	0.143
Tortuosity grade	0.103	0.431	0.048	0.706	−0.171	0.169	−0.196	0.130
Beading frequency	−0.267	0.024	0.243	0.038	−0.031	0.804	0.197	0.115
PT-INR	0.359	0.002	−0.217	0.144	−0.305	0.010	−0.028	0.821
APTT	0.279	0.025	−0.202	0.094	−0.159	0.221	0.195	0.128
Fibrinogen	−0.078	0.516	0.181	0.194	0.493	0.0001	−0.001	0.995

APTT, activated partial thromboplastin time; BMI, body mass index; CEBC, corneal epithelial basal cell; CV, coefficient of variation; PT-INR, prothrombin time international normalizing ratio; SBP, systolic blood pressure.

area in control subjects in the present study was 17.1%, which was quite similar to a previous report[18]. The width of intercellular spaces between neighboring CEBCs in culture condition, as observed by scanning electron microscopy, was previously reported as 1.0–1.5 μm[19], which was slightly narrower than that (2.21 ± 0.02 μm) observed in our controls. The difference might be explained by differences between *in vivo* and *in vitro* fixed samples or differences between microscopy and electron microscopy. Therefore, the determination of morphometric features of CEBCs using CCM in the present study was considered to be appropriate.

As per our knowledge, the influence of diabetes on CEBC area and area variability, as well as on the width of the intercellular space between neighboring CEBCs, has never been reported. The present study showed that CEBCs were smaller, had lower density, were more variable in area and had wider intercellular spaces in type 2 diabetics than in controls. Lower CEBC density in patients with type 2 diabetes had also been documented in previous reports[9,10]. When normal human CEBCs were cultured in a normal (6 mmol/L) or high (30 mmol/L) glucose environment for 14 days, cell density and [^{3}H]-thymidine incorporation under the high glucose condition decreased compared with those under the normal glucose condition[20]. Therefore, *in vivo* or *in vitro* hyperglycemic conditions result in a lower density of CEBC. Diabetes-associated corneal alterations include increased basement membrane thickness[21]. Wider intercellular spaces between neighboring CEBCs in patients with diabetes might be attributed to a higher rate of cell death and regeneration caused by focal degeneration of CEBCs[22]. Excessively rapid differentiation and maturation can also contribute to CEBC area variability.

Corneal nerve bundles subdivide into smaller bundles and perforate Bowman's layer and the basal layer of the corneal epithelium, where they divide again. From there, the individual NF merges toward the superficial layers of the corneal epithelium[23]. NFs have an important influence on corneal nutrition and contribute to the maintenance of a healthy corneal surface. Alterations in corneal innervation produce neurotrophic keratopathy[7,24]. By quantifying small fiber pathological changes using the technique of intraepidermal nerve fiber (IENF) assessment, as well as CCM in 54 diabetic patients stratified for DN, Quattrini *et al.*[25] showed that whereas both techniques of CCM and IENF assessment accurately reflect the severity of somatic neuropathy, CCM detects damage before detectable nerve dysfunction, suggesting the superiority of CCM over IENF. Tavakoli *et al.*[26] reported that CNFD, CNFL and CNBD decreased significantly with increasing severity of DN, and concluded that CCM might be used to detect early nerve damage. Recently, the parameter of CCM which best identifies DN in type 1 diabetes was investigated by Ahmed *et al.*[27]. They suggested that the measurement of CNFL offers optimized sensitivity and specificity for ruling out DN. Therefore, we analyzed the morphometric features of the sub-basal nerve plexus of controls and type 2 diabetic patients. Similar to the aforementioned investigations, before developing DN, type 2 diabetic patients showed decreased CNFD, CNFL, CNBD and beading

frequency, and exaggerated tortuosity. The development of DN further decreased CNFD and CNFL, and increased tortuosity.

According to a previous report[10], lower CEBC density was significantly and directly correlated with CNFD and CNBD, whereas it was inversely correlated with tortuosity grade in modestly controlled type 2 diabetic patients. However, the influence of beading frequency on the CEBC morphology has never been studied. In contrast to a previous report, the present study showed that among parameters of corneal nerve plexus, beading frequency was the single possible independent predictor of CEBC density and area. The beading can be clearly shown along corneal NFs by CCM, and it coincides with the accumulation of mitochondria observed by electron microscopic examination of the cornea[6]. The mitochondria in neurons play a pivotal role in supplying sufficient energy for transmitting signals that allow the maintenance of function and morphology of innervated tissues. Therefore, decreased beading as a result of hyperglycemia might alter CEBC density and size in addition to the direct influence of hyperglycemia on CEBCs, as evidenced by *in vitro* culture under hyperglycemic conditions[19]. However, we could not determine whether beading primarily influences CEBC density or area. Because we carried out multiple regression analysis for four outcome variables of morphometric parameters of CEBCs, the Bonferroni correction for *P*-values might be indicated to avoid a false positive relationship. If the Bonferroni correction was made, a significant *P*-value should be $<0.5/4 = 0.125$. Then, the relationship between beading frequency and density or area of CEBCs lost significance, suggesting that the regulatory role of beading frequency on morphology of CEBCs might be spurious. Previously, we reported that beading frequency reflects HbA_{1c} levels of the preceding 1–3 months in type 1[12] and type 2 diabetes[28]. Because diabetic participants in the present study were visiting our clinic for the first time under poor glycemic control (HbA_{1c} 9.1%), the hyperglycemia-induced reduction in beading frequency might attenuate the relationship to morphology of CEBCs. Further studies after glycemic control are warranted to establish the definite relationship between corneal NF pathology and features of CEBCs.

Finally, the clinical factors predisposing to morphological changes in CEBCs in type 2 diabetic patients were examined. A longer duration of diabetes decreased CEBC size, led to an exaggerated blood coagulation state as judged by lower PT-INR and APTT, and decreased CEBC density, whereas a higher fibrinogen level contributed to increased area variability. We could not identify the clinical factors influencing the intercellular space between neighboring CEBCs. Inoue *et al.*[11] examined the contribution of ocular and systemic factors to diabetic keratoepitheliopathy by multiple regression analysis, and concluded that qualitative abnormalities in tear secretion seemed relevant to the development of diabetic keratoepitheliopathy. However, they could not ascertain the contribution of systemic factors, such as the duration of diabetes and HbA_{1c} levels. Furthermore, they did not examine the influence of coagulation status on diabetic keratoepitheliopathy. The positive correlation between coagulation state and morphology of CEBCs in non-diabetic controls strengthens the role of exaggerated coagulation state in the impaired morphology of CEBCs in type 2 diabetic patients. Because the present study did not evaluate keratoepitheliopathy, the elucidation of mechanisms by which an exaggerated coagulation state contributes to diabetic keratoepitheliopathy through the deranged CEBCs was beyond the scope of our study. However, previous investigations[29,30] suggested the etiological role of components of the coagulation cascade in developing keratoepitheliopathy. In plasminogen deficient mice[29], corneal wound healing was markedly impaired, whereas mice lacking fibrinogen or plasminogen and fibrinogen showed normal corneal wound healing after epithelial ablation. These observations indicate that the impaired corneal wound healing in plasminogen deficient mice is mechanistically related to fibrinogen. The absence of plasmin-mediated fibrin clearance results in fibrin deposition, and secondary adverse inflammatory reactions. The authors suggested the pathogenetic role of fibrinogen in delayed corneal wound healing[29]. The deposited fibrinogen and other plasma products within the corneal wound seem to derive from tears. The expression of plasminogen activators by corneal epithelial cells suggests that the coagulation and fibrinolytic systems play an important role in corneal wound healing.

An *in vitro* study[30] using human cornea showed the presence of components (prothrombin and fibrinogen) of the coagulation cascade in the cornea. These components were found in the whole cornea, as evidenced by the presence of their proteins and messenger ribonucleic acid, being highest in basal cells. A cleavage of fibrinogen to fibrin by thrombin results in corneal opacity, and thrombin regulates corneal wound healing by regulating growth factor, cytokines and extracellular matrix. Therefore, upregulation of the coagulation cascade in the cornea (CEBCs) in diabetes might be one of the causative mechanisms in keratoepitheliopathy. Because the cornea was donated from a cadaver, the parallelism of these components between cornea and plasma had never been examined. However, the exaggerated coagulation state in type 2 diabetes might play some role in the development of diabetic keratoepitheliopathy, although our study did not assess coagulation factors in the cornea.

There was no difference in the morphometric features of CEBCs and beading frequency of corneal NF between type 2 diabetic patients with DN and those without. As we pointed out, beading frequency is only one possible regulator of CEBC density and area. In contrast, using Goto–Kakizaki rats (non-obese animal model of type 2 diabetes similar to Japanese type 2 diabetes), Wang *et al.*[31] showed the concomitant presence of a decreased corneal NF density visualized by CCM, reduced corneal sensitivity and tear secretion, and delayed epithelial wound healing and re-innervation, suggesting that diabetic neuropathy is linked to delayed wound healing in the cornea (keratoepitheliopathy). However, they did not document beading frequency, the morphology of CEBCs, nor did they analyze the direct relationships among delayed epithelial repair,

re-innervation and the degree of hyperglycemia. Therefore, the direct interrelationship among the features of CEBCs, corneal innervation and diabetic keratoepitheliopathy remains to be fully clarified.

In conclusion, CCM showed that CEBCs in type 2 diabetic patients are sparser, smaller, more variable in size and have wider intercellular spaces compared with CEBCs of controls. Although our data showed that decreased beading in corneal nerve plexus, accelerated coagulation state and longer duration of diabetes might be contributing factors for the observed alterations in morphometric features of CEBCs in type 2 diabetic patients, we acknowledge many limitations to the interpretation of the present results. First, because we did not measure corneal functions, such as tear secretion (dry eyes) and corneal sensitivity, nor did we evaluate corneal health or keratoepitheliopathy, we could not evaluate the contribution of impaired corneal function to CEBC pathology, nor clarify the relationship between CEBC pathology and the occurrence or severity of keratoepitheliopathy. Second, because the relationship between corneal NF pathology and morphology of CEBCs might be spurious, further study after glycemic control should be carried out. Third, as we focused on morphology of CEBCs, but not on corneal function, the present study could not clarify their influence on each other. Fourth, as with previous studies, we could not find a relationship between the features of CEBCs and the degree of hyperglycemia (HbA_{1c} level). Therefore, the direct impact of hyperglycemia on the morphology of CEBCs remained to be clarified. Finally, our data were cross-sectional under hyperglycemic conditions. A longitudinal study carrying out a CCM examination of CEBCs and corneal NFs before and after glycemic control would provide more vigorous data regarding the relationship between the morphometric changes of CEBCs, and the contributing corneal nerve pathology and the clinical factors.

ACKNOWLEDGEMENTS

The present study received no financial support. None of the authors have any potential conflicts of interest to disclose.

REFERENCES

1. Didenko TN, Smoliakova GP, Sorokin EL, *et al.* Clinical and pathogenetic features of neurotrophic corneal disorders in diabetes. *Vestn Oftalmol* 1999; 115: 7–11 (Russian).
2. Schultz RO, Van Horn DL, Peters MA, *et al.* Diabetic keratopathy. *Trans Am Ophthalmol Soc* 1981; 79: 180–199.
3. Schultz RO, Matsuda M, Yee RW, *et al.* Corneal endothelial changes in type I and type II diabetes mellitus. *Am J Ophthalmol* 1984; 98: 401–410.
4. Herse PR. A review of manifestations of diabetes mellitus in the anterior eye and cornea. *Am J Optom Physiol Opt* 1988; 65: 224–230.
5. Foulks GN, Thoft RA, Perry HD, *et al.* Factors related to corneal epithelial complications after closed vitrectomy in diabetics. *Arch Ophthalmol* 1979; 97: 1076–1078.
6. Müller LJ, Pels L, Vrensen GF. Ultrastructural organization of human corneal nerves. *Invest Ophthalmol Vis Sci* 1996; 37: 476–488.
7. Castillo JM, Acosta MC, Wassfi MA, *et al.* Relation between corneal innervation with confocal microscopy and corneal sensitivity with noncontact esthesiometry in patients with dry eye. *Invest Ophthalmol Vis Sci* 2007; 48: 173–181.
8. Yoon KC, Im SK, Seo MS. Changes of tear film and ocular surface in diabetes mellitus. *Korean J Ophthalmol* 2004; 18: 168–174.
9. Quadrado MJ, Popper M, Morgado AM, *et al.* Diabetes and corneal cell densities in humans by in vivo confocal microscopy. *Cornea* 2006; 25: 761–768.
10. Chang PY, Carrel H, Huang JS, *et al.* Decreased density of corneal basal epithelium and subbasal corneal nerve bundle changes in patients with diabetic retinopathy. *Am J Ophthalmol* 2006; 142: 488–490.
11. Inoue K, Kato S, Ohara C, *et al.* Ocular and systemic factors relevant to diabetic keratoepitheliopathy. *Cornea* 2001; 20: 798–801.
12. Ishibashi F, Okino M, Ishibashi M, *et al.* Corneal nerve fiber pathology in Japanese type 1 diabetic patients and its correlation with antecedent glycemic control and blood pressure. *J Diabetes Invest* 2012; 3: 191–198.
13. Oliveira-Soto L, Efron N. Morphology of corneal nerves using confocal microscopy. *Cornea* 2001; 20: 374–384.
14. Japanese Study Group of Diabetic Neuropathy. Simplified diagnostic criteria for diabetic neuropathy (distal symmetric polyneuropathy). *Peripher Nerv* 2001; 12: 225–227 (Japanese).
15. Kashiwagi A, Kasuga M, Araki E, *et al.* International clinical harmonization of glycated hemoglobin in Japan: From Japan Diabetes Society to Glycohemoglobin Standardization Program Values. *J Diabetes Invest* 2012; 3: 39–40.
16. Shimazaki J, Shimmura S, Mochizuki K, *et al.* Morphology and barrier function of the corneal epithelium after penetrating keratoplasty: association with original diseases, tear function, and suture removal. *Cornea* 1999; 18: 559–564.
17. Harrison DA, Joos C, Ambrosio R. Morphology of corneal basal epithelial cells by in vivo slit-scanning confocal microscopy. *Cornea* 2003; 22: 246–248.
18. Gaujoux T, Touzeau O, Laroche L, *et al.* Morphometry of corneal epithelial cells on normal eyes and after anterior lamellar keratoplasty. *Cornea* 2010; 29: 1118–1124.
19. Koizumi N, Cooper LJ, Fullwood NJ, *et al.* An evaluation of cultured corneal limbal epithelial cells, using cell-suspension culture. *Invest Ophthalmol Vis Sci* 2002; 43: 2114–2121.
20. Fujita H, Morita I, Takase H, *et al.* Prolonged exposure to high glucose impaired cellular behavior of normal human corneal epithelial cells. *Curr Eye Res* 2003; 27: 197–203.
21. Sanchez-Thorin JC. The cornea in diabetes mellitus. *Int Ophthalmol Clin* 1998; 38: 19–36.
22. Vracko R. Basal lamina layering in diabetes mellitus. Evidence for accelerated rate of cell death and cell regeneration. *Diabetes* 1974; 23: 94–104.

23. Müller LJ, Marfurt CF, Kruse F, *et al*. Corneal nerves: structure, contents and function. *Exp Eye Res* 2003; 76: 521–542.
24. Bikbova G, Oshitari T, Tawada A, *et al*. Corneal changes in diabetes mellitus. *Curr Diabetes Rev* 2012; 8: 294–302.
25. Quattrini C, Tavakoli M, Jeziorska M, *et al*. Surrogate marker of small fiber damage in human diabetic neuropathy. *Diabetes* 2007; 56: 2148–2154.
26. Tavakoli M, Finnigan J, Quattrini C, *et al*. Corneal confocal microscopy. *Diabetes Care* 2010; 33: 1792–1797.
27. Ahmed A, Bril V, Orszag A, *et al*. Detection of diabetic sensorimotor polyneuropathy by corneal confocal microscopy in type 1 diabetes: a concurrent validity study. *Diabetes Care* 2012; 35: 821–828.
28. Ishibashi F. Glycemic state has real-time impact on beading size and frequency while requiring several years to influence nerve fibers by corneal confocal microscopy. *Diabetes* 2012; 61(Suppl.1): A148.
29. Kao WWY, Kao CWC, Kaufman AH, *et al*. Healing of corneal epithelial defects in plasminogen- and fibrinogen-deficient mice. *Invest Ophthalmol Vis Sci* 1998; 39: 502–508.
30. Ayala A, Warejcka DJ, Olague-Marcban M, *et al*. Corneal activation of prothrombin to form thrombin, independent of vascular injury. *Invest Ophthalmol Vis Sci* 2007; 48: 134–143.
31. Wang F, Gao N, Yin J, *et al*. Reduced innervation and delayed re-innervation after epithelial wounding in type 2 diabetic Goto-Kakizaki rats. *Am J Pathol* 2012; 181: 2058–2066.